

Quantum quench dynamics in the transverse field Ising model at nonzero temperatures

Nils O. Abeling* and Stefan Kehrein

Institut für Theoretische Physik, Georg-August-Universität Göttingen, Friedrich-Hund-Platz 1, 37077 Göttingen, Germany

(Received 16 November 2015; revised manuscript received 19 February 2016; published 11 March 2016)

The recently discovered *dynamical phase transition* denotes nonanalytic behavior in the real-time evolution of quantum systems in the thermodynamic limit, and it has been shown to occur in different systems at zero temperature [Heyl *et al.*, *Phys. Rev. Lett.* **110**, 135704 (2013)]. In this paper, we extend the analysis to nonzero temperature by studying a generalized form of the Loschmidt echo, the work distribution function, of a quantum quench in the transverse field Ising model. Although the quantitative behavior at nonzero temperatures still displays features derived from the zero-temperature nonanalyticities, it is shown that in this model dynamical phase transitions do not exist if $T > 0$. This is a consequence of the system being initialized in a thermal state. Moreover, we elucidate how the Tasaki-Crooks-Jarzynski relation can be exploited as a symmetry relation for a global quench or to obtain the change of the equilibrium free-energy density.

DOI: [10.1103/PhysRevB.93.104302](https://doi.org/10.1103/PhysRevB.93.104302)

I. INTRODUCTION

Recent experimental advances in studying closed quantum systems using cold atomic gases in optical lattices have spurred interest and activity in the field of nonequilibrium dynamics [1–3]. The experiments benefit from both the high controllability and time resolution of these systems and the possibility to realize different initial states. With this experimental setup at hand, we can now address fundamental questions of quantum many-body physics concerning thermalization and the influence of integrability. The simplest procedure to drive a system into nonequilibrium is a *quantum quench*, i.e., a sudden change of the Hamiltonian $H(g)$ with only short-range interactions to $H(g')$, where g denotes the altered parameter, e.g., the change of an external magnetic field. Having prepared the system with respect to the original Hamiltonian $H(g)$ (often in the ground state), the unitary time evolution with the quenched Hamiltonian is nontrivial since it starts with a nonthermal superposition of eigenstates. For a more general ramp protocol λ , the set of system parameters at the specific time t is denoted by λ_t .

To study quench dynamics, one can analyze an experimentally tractable quantity: the performed work. Unlike equilibrium quantities such as the free energy, the *inclusive* work W given by the difference of two consecutive energy measurements, i.e.,

$$W = E_m^{\lambda_\tau} - E_n^{\lambda_0},$$

is well-defined in nonequilibrium [4]. Here, λ_τ and λ_0 denote the system parameters at the respective times of the energy measurements, which yielded the eigenvalues E_n and E_m in their instantaneous eigenbasis. At nonzero temperature, the work depends not only on the entire ramp protocol λ , but also on the initial distribution of states, and therefore it is a stochastic variable with a probability distribution. For this function, which is known as the work distribution function (WDF), important theorems describing the fluctuations have been found, namely the famous Jarzynski equality and its generalization, the Tasaki-Crooks relation [5]. However, due to the fragility of quantum systems toward the environment and a

potential collapse of the wave function, the theorems have been mostly studied and tested for classical microscopic systems, e.g., the stretched RNA experiment [6–8]. It was only very recently that An *et al.* verified the quantum Jarzynski equality with a trapped-ion system [9].

In this work, we calculate the work distribution function for different global ramp protocols and test the Tasaki-Crooks relation, thereby predicting the equilibrium quantity, i.e., the change of the free-energy density of the corresponding equilibrium states. Another motivation to study the work distribution function arises when a double quench protocol has been implemented (sketched in Fig. 1). It denotes a quench where the initial and final Hamiltonian are identical while the time evolution is governed by $H(g')$, i.e., with a changed parameter $g \rightarrow g'$. In this case, the Loschmidt echo defined as $\mathcal{L}(t) = |\mathcal{G}(t)|^2$ is intrinsically contained in the work distribution function at $T = 0$. Here, the overlap or return probability amplitude

$$\mathcal{G}(t) = \langle \psi | e^{-iH(g')t} | \psi \rangle \quad (1)$$

represents the probability amplitude to recover the initial state $|\psi\rangle$ after the quench. In principle, the initial state can be any state, but it is often chosen to be the ground state [10]. In other words, the Loschmidt echo measures how much the system is affected by the perturbing quench. At the same time, however, the echo represents the probability density that no work is performed on the system during the double quench, since the final and the initial state are identical. The work distribution function can therefore be regarded as a generalization of the Loschmidt echo, since it also contains the realizations that the system ends up in a different (excited) state and energy is added or extracted [11].

As a consequence of the aforementioned close relation, the work distribution function shares the features of the Loschmidt echo, such as the newly discovered dynamical phase transition (DPT), which describes nonanalytic behavior in the time evolution (cf. Sec. III C) [10]. This phenomenon was first observed studying the Loschmidt echo at $T = 0$, but it was also shown to appear naturally in the work distribution function by Heyl *et al.* Since the initial paper, the DPT has been the focus of numerous studies that showed that this phenomenon also

*nils.abeling@theorie.physik.uni-goettingen.de

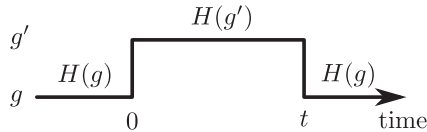


FIG. 1. Sketch of a double quench: At $t = 0$ the parameter g is quenched to g' such that the Hamiltonian $H(g')$ governs the nontrivial time evolution. At t the system is quenched back.

emerges in nonintegrable models [12,13], and which treated the conditions under which they occur [14,15]. Other advances addressed the question of how one can further classify a DPT and how it arises in the context of DMFT [16]. Moreover, it was analyzed how local contributions affect the dynamical free energy and therefore the DPT [17], while other works revealed a connection of the DPT to the order parameter dynamics in systems with broken-symmetry phases [18]. Due to the close analogy to equilibrium phase transitions, a recent development also deals with questions of universality and scaling [19].

The purpose of this paper is to investigate the quench dynamics for single and double quench protocols of the transverse field Ising model at nonzero temperature, i.e., the effect of the initial state being not the ground state but a thermal state. In addition to the analysis of the corresponding rate functions and the application and verification of the Tasaki-Crooks-Jarzynski theorem, we study whether the DPT survives the change to nonzero temperatures. The procedure starts with the analytic calculation of the characteristic function of work, which can then be transformed to the work distribution function by applying the Gärtner-Ellis theorem, as explained in Sec. II. In Sec. III, we briefly introduce the model, i.e., the transverse field Ising model in one dimension, and how it is solved. We then display the actual calculation of the characteristic function of work for both the single and the double quench protocol. The results for the rate functions of the work distribution functions are displayed and discussed in Sec. IV. Finally, the previous results are used to verify the Tasaki-Crooks theorem for a global quench for the implemented system at nonzero temperature. In addition, we demonstrate how the relation can serve as a powerful tool to either determine a change in the free-energy density or to relate different parts of the entire work distribution function in Sec. V.

II. THE CHARACTERISTIC FUNCTION OF WORK

Since work is a stochastic variable in microscopic systems, it is necessary to consider its probability density function, the so-called work distribution function. If the principle of microreversibility holds, i.e., if the Hamiltonian is time reversal invariant at any time t , the only remaining ingredient for the formal definition of the work distribution function is the initial probability distribution of states p_n^0 (e.g., the canonical distribution) [5,20]. Having defined the probability to transition from state n into m (also called conditional probability) $p_{m|n}$, which depends on the ramp protocol λ , the work distribution function is given as the product of the two

probabilities and reads

$$p[W; \lambda] = \sum_{m,n} \delta(W - (E_m^{\lambda_\tau} - E_n^{\lambda_0})) p_{m|n}[\lambda] p_n^0. \quad (2)$$

The square brackets emphasize the functional dependence on the ramp protocol λ . For complicated ramp protocols, the calculation of the WDF can be cumbersome because the eigenbasis changes during the quench. While some generic protocols have been studied [21], the expression simplifies significantly for single or double quenches.

Instead of directly calculating the WDF in Eq. (2), it is often easier to first determine its generating function, the characteristic function of work $G[u; \lambda]$, defined as the Fourier transform

$$G[u; \lambda] = \int dW e^{iuW} p[W; \lambda] \quad (3)$$

with $u \in \mathbb{C}$. With $u = iR$, $R \in \mathbb{R}$, the work distribution function then results from a saddle-point approximation of the inverse Laplace transformation of $G(R)$. This is achieved by the Gärtner-Ellis theorem in the context of large deviation theory, as explained in Sec. IV.

The reason to focus on this procedure is the possibility to analytically calculate the characteristic function of work. It was shown by Talkner *et al.* [4] that $G[u; \lambda]$ can be written as a time-ordered exponential function of exponentiated Hamiltonians as

$$\begin{aligned} G[u; \lambda] &= \langle e^{iuH_t^H(\lambda_\tau)} e^{-iuH(\lambda_0)} \rangle \\ &= \frac{1}{Z(\lambda_0)} \text{Tr} (e^{iuH_t^H(\lambda_\tau)} e^{-(iu+\beta)H(\lambda_0)}). \end{aligned} \quad (4)$$

Here, $H_t^H(\lambda_t) = U_{t,0}^\dagger[\lambda] H(\lambda_t) U_{t,0}[\lambda]$ denotes the Hamiltonian in the Heisenberg picture at time t . The unitary operator $U_{t,0}[\lambda]$ is the usual time evolution operator, which depends on the ramp protocol.

For a single quench, the equation above can be simplified further, since $H(t < 0) = H(g)$ and $H(t \geq 0) = H(g')$ without any time evolution. It follows that

$$G(u) = \frac{1}{Z(g)} \text{Tr} (e^{iuH(g')} e^{-(iu+\beta)H(g)}). \quad (5)$$

At zero temperature, the difference of the ground-state energies $W_{\min} = E_0(g') - E_0(g)$ is the minimal work that can be measured. It is therefore convenient to shift the scale such that $W_{\min} = 0$ and $p(W < 0) = 0$. To be able to compare the $T > 0$ results to the $T = 0$ case, we make the same adjustment for the nonzero temperature calculations.

When the ramp protocol is chosen to have a double quench form, Eq. (4) yields

$$\begin{aligned} G(u, t) &= \langle U_{t,0}^\dagger(g') e^{iuH(g)} U_{t,0}(g') e^{-iuH(g)} \rangle \\ &= \frac{1}{Z(g)} \text{Tr} (e^{itH(g')} e^{iuH(g)} e^{-itH(g')} e^{-(iu+\beta)H(g)}), \end{aligned} \quad (6)$$

because the unitary time evolution is now determined by the quenched Hamiltonian. As the quenches we consider describe *global* quenches, i.e., every single site is affected, the measured work will grow extensively with system size N . The quantity that remains finite is therefore the intensive work density $w = W/N$, which changes the definition of the characteristic

function of work in Eq. (3) to

$$G(u) = \int dw e^{iuwN} p(w) = \langle e^{iuwN} \rangle. \quad (7)$$

III. THE TRANSVERSE FIELD ISING MODEL

The model that is studied is the exactly solvable transverse field Ising model in one dimension given by the Hamiltonian

$$H(g) = -\frac{1}{2} \sum_{l=1}^{N-1} \sigma_l^z \sigma_{l+1}^z + \frac{g}{2} \sum_{l=1}^N \sigma_l^x \quad (8)$$

with periodic boundary conditions (PBCs). It describes a lattice with N spin-1/2 particles that experience next-neighbor interaction with an overall external magnetic field proportional to g . The system features a quantum phase transition at the critical magnetic field $g = g_c = 1$. This point separates the quantum paramagnetically ordered phase ($g > 1$) from the regime where ferromagnetic ordering occurs ($g < 1$). To solve the model, the Hamiltonian is mapped to a fermionic model via a Jordan-Wigner transformation [22,23], which leads to a form in which the Hamiltonian is split into different independent momentum sectors such that $H = \sum_{0 < k < \pi} H_k$ with

$$H_k = (c_k^\dagger \quad c_{-k}) \begin{pmatrix} g - \cos k & -i \sin k \\ i \sin k & -(g - \cos k) \end{pmatrix} \begin{pmatrix} c_k \\ c_{-k}^\dagger \end{pmatrix}. \quad (9)$$

The momentum index k is set by the PBC to be $k = \frac{2\pi}{N}m$, $m \in \mathbb{Z}$. An additional constant term is ignored, since it does not affect the physics. The matrix is diagonalized by a fermionic Bogoliubov transformation

$$\begin{pmatrix} c_k \\ c_{-k}^\dagger \end{pmatrix} = \begin{pmatrix} \cos \theta & i \sin \theta \\ i \sin \theta & \cos \theta \end{pmatrix} \begin{pmatrix} \eta_k \\ \eta_{-k}^\dagger \end{pmatrix} \quad (10)$$

with $\tan 2\theta = \sin k / (g - \cos k)$ to yield

$$H = \sum_{0 < k < \pi} \epsilon_k(g) (\eta_k^\dagger \eta_k - \eta_{-k} \eta_{-k}^\dagger) \quad (11)$$

with the dispersion relation $\epsilon_k(g) = \sqrt{(g - \cos k)^2 + \sin^2 k}$.

From Eq. (11), one learns that each sub-Hilbert space describes a three-level system consisting of the lowest state without any fermions $|0_k\rangle$ and energy $-\epsilon_k(g)$; a twofold-degenerate singly occupied state $|1_{\pm k}\rangle$ with one fermion with momentum k or $-k$, respectively, and zero energy; and a fully occupied state $|2_k\rangle$ containing both fermions and energy $\epsilon_k(g)$.

The Bogoliubov transformation can also be used to calculate the quenches. Depending on the system parameter, the eigenbasis changes over the course of the ramp protocol such that one needs to translate the new eigenstates in terms of the previous eigenstates. Due to momentum conservation, the singly occupied eigenstates do not change, whereas the unoccupied and fully occupied states transform via a linear

superposition according to

$$|0_k(g)\rangle = (\cos \phi_k + i \sin \phi_k \eta_k^\dagger(g') \eta_{-k}^\dagger(g')) |0_k(g')\rangle, \quad (12)$$

$$|2_k(g)\rangle = (i \sin \phi_k + \cos \phi_k \eta_k^\dagger(g') \eta_{-k}^\dagger(g')) |0_k(g')\rangle, \quad (13)$$

where ϕ_k denotes the Bogoliubov angle $\phi_k = \theta(g) - \theta(g')$.

A. Single quench

The method to calculate the WDF for a single quench uses the characteristic function of work in Eq. (5). Exploiting the simple k -sector form of the Hamiltonian, one finds for the single quench that

$$\begin{aligned} G(u) &= \frac{1}{Z(g)} \text{Tr} \left(e^{iu \sum_{0 < k < \pi} H_k(g')} e^{-(iu+\beta) \sum_{0 < k < \pi} H_k(g)} \right) \\ &= \frac{1}{Z(g)} \prod_{0 < k < \pi} \text{Tr}_k \left(e^{iu H_k(g')} e^{-(iu+\beta) H_k(g)} \right), \end{aligned} \quad (14)$$

where the partial trace Tr_k only runs over the four eigenstates $|i_k\rangle$ of a k -sector. The last step that rearranges the different H_k becomes possible because $[H_k(g), H_{k'}(g')] = 0$ if $k \neq k'$. With $Z(g) = \text{Tr} e^{-\beta H(g)} = \prod_{0 < k < \pi} \text{Tr}_k e^{-\beta H_k(g)}$, one obtains

$$\begin{aligned} G(u) &= \prod_{0 < k < \pi} \frac{1}{Z_k(g)} \sum_{i_k} e^{-(iu+\beta) E_{i_k}(g)} \\ &\quad \times \langle i_k(g) | e^{iu H_k(g')} | i_k(g) \rangle. \end{aligned} \quad (15)$$

One way to calculate the explicit form of the equation above is to express the quenched basis states in terms of the original ones via Eqs. (12) and (13). Since the singly occupied states with zero energy do not change, $\langle 1_{\pm k}(g) | e^{iu H_k(g')} | 1_{\pm k}(g) \rangle = 1$. For the remaining two states, one finds

$$\begin{aligned} \langle 0_k(g) | e^{iu H_k(g')} | 0_k(g) \rangle &= \cos[u\epsilon_k(g')] \\ &\quad - i \cos(2\phi_k) \sin[u\epsilon_k(g')], \end{aligned} \quad (16)$$

$$\begin{aligned} \langle 2_k(g) | e^{iu H_k(g')} | 2_k(g) \rangle &= \cos[u\epsilon_k(g')] \\ &\quad + i \cos(2\phi_k) \sin[u\epsilon_k(g')] \end{aligned} \quad (17)$$

such that eventually

$$G(u) = \prod_{0 < k < \pi} G_k(u)$$

with

$$\begin{aligned} G_k(u) &= \left[\frac{1 + \cosh[(iu + \beta)\epsilon_k(g)] \cos[u\epsilon_k(g')]}{1 + \cosh[\beta\epsilon_k(g)]} \right. \\ &\quad \left. - i \frac{\sinh[(iu + \beta)\epsilon_k(g)] \cos(2\phi_k) \sin[u\epsilon_k(g')]}{1 + \cosh[\beta\epsilon_k(g)]} \right] \end{aligned} \quad (18)$$

with the partition function for a single mode $Z_k(g) = \sum_{i_k} e^{-\beta E_{i_k}(g)} = 2\{1 + \cosh[\beta\epsilon_k(g)]\}$.

B. Double quench

The characteristic function for the double quench protocol is calculated in a similar manner, since a double quench consists of two single quenches and a unitary time

evolution for time t in between. However, this makes it necessary to translate the basis states twice, and one finally evaluates Eq. (6) to result in $G(u, t) = \prod_{0 < k < \pi} G_k(u, t)$ with

$$G_k(u, t) = \frac{1 + \cosh[\beta \epsilon_k(g)] (\cos^2[t \epsilon_k(g')] + \cos^2(2\phi_k) \sin^2[t \epsilon_k(g')] + \sin^2(2\phi_k) \sin^2[t \epsilon_k(g')] \cosh[(2iu + \beta) \epsilon_k(g)]}{1 + \cosh[\beta \epsilon_k(g)]}. \quad (19)$$

C. The dynamical phase transition at $T = 0$

In the previous sections, it was shown how the work distribution function is related to the characteristic function of work for a general complex u and how it can be calculated for the one-dimensional transverse field Ising model. To see how the DPT appears in the work distribution function, one first has to understand the connection to the Loschmidt echo.

One way follows a similar path as the derivation by Heyl *et al.* in their original paper [10]. Motivated by the similarity between the canonical partition function of an equilibrium system $Z(\beta) = \text{Tr} e^{-\beta H}$ and the Loschmidt overlap, they studied the boundary partition function

$$Z(z) = \langle \psi_0 | e^{-zH} | \psi_0 \rangle \quad (20)$$

with $z \in \mathbb{C}$ and $|\psi_0\rangle$ denoting the ground state. This expression represents the Loschmidt overlap when $z = it$, i.e., on the imaginary axis. Due to exponential scaling with system size, this quantity takes on a large deviation form $Z(z) \sim e^{-Nf(z)}$ in the thermodynamic limit such that one defines the free-energy density

$$f(z) = - \lim_{N \rightarrow \infty} \frac{1}{N} \ln Z(z), \quad (21)$$

where N is the system size. Analogously to equilibrium phase transitions where nonanalytic behavior of the free-energy density results from zeros of the partition function in the complex temperature plane, Heyl *et al.* showed that a similar phenomenon occurs when analyzing the dynamics of the Loschmidt overlap. In the thermodynamic limit, the zeros of the boundary partition function, the so-called *Fisher zeros*, coalesce into lines, which cross the time axis under certain conditions [10]. This leads to nonanalytic behavior in the free-energy density, which is just the rate function of the Loschmidt overlap at critical times t_n^* with

$$t_n^* = \frac{\pi}{E_{k^*}(g')} \left(n + \frac{1}{2} \right), \quad n = 0, 1, 2, \dots, \quad (22)$$

where the dispersion relation is given by $E_k(g)$ and k^* is determined by $\cos k^* = (1 + gg')/(g + g')$. The close analogy to equilibrium phase transitions inspired the authors to call this phenomenon the *dynamical phase transition*. In the Introduction, we argued that the Loschmidt echo can be identified with the work distribution function for a double quench where no work is performed on the system, i.e., $p(w = 0)$. Therefore, the DPT also appears as nonanalytic behavior in the corresponding rate function $r(w, t)$ of the work distribution function [10].

Another way to recognize the close relation between the Loschmidt echo and the work distribution function is to analyze the characteristic function of work $G(u)$. If, for example, one considers a single quench that requires two energy measurements in order to determine the work, then

the corresponding characteristic function of work is given by Eq. (5). Taking the zero-temperature limit $\beta \rightarrow \infty$ reduces the trace over all states to a single term with the ground state, such that one ends up with

$$G(u) = \langle \psi_0 | e^{iu[H(g') - E_0(g)]} | \psi_0 \rangle. \quad (23)$$

It readily follows with $u = t$ that $G(t) = \mathcal{L}(t)^*$, where the energy scale of $H(g')$ has been shifted by the constant ground-state energy $E_0(g)$ [11]. This shift is a remnant of the definition of the work distribution function in Eq. (2), where $E_n^{\lambda_0}$ was not set to 0 for $n = 0$.

As the work distribution function treats all possible measurement outcomes, it is more difficult to relate the general double quench WDF to the Loschmidt echo. From the previous considerations, one assumes a connection to the case in which no work is performed ($W = 0$) in the zero-temperature limit. The easiest way to establish the link is to start with the general WDF in Eq. (2) where the time evolution is contained within the transition probability $p_{m|n}$, and to perform the zero-temperature limit $\beta \rightarrow \infty$ ($\lambda_\tau = \lambda_0 = g$). The limit simplifies the initial distribution of states $p_n^0 = \delta_{n0}$, where only the ground state ($n = 0$) survives. With $p_{m|n} = |\langle E_m(g) | e^{-iH(g')t} | E_n(g) \rangle|^2$, this finally yields

$$p(W, t) = \sum_m \delta(W - [E_m(g) - E_0(g)]) \times |\langle E_m(g) | e^{-iH(g')t} | E_0(g) \rangle|^2. \quad (24)$$

For $W = 0$, the equation further reduces to the Loschmidt echo $\mathcal{L}(t)$ demonstrating the close relation of the two quantities. Therefore, we expect that any nonanalytic behavior in the rate function of $\mathcal{L}(t)$ can be found by studying the dynamics of the rate function of the work distribution function.

IV. THE WORK DISTRIBUTION FUNCTION

In the preceding section, the characteristic function of work was calculated for both the single and double quench. Now, in the last step, one needs to calculate the WDF. Similar to the boundary partition function, the work distribution function $p(w)$ is expected to show large deviation behavior, i.e., $p(w) \propto e^{-Nr(w)}$, with some non-negative rate function $r(w)$ [24]. Besides giving the mean value \bar{w} , where $r(\bar{w}) = 0$ and thus $p(\bar{w})$ is maximal, the rate function provides additional information about fluctuations in its tails. The underlying theory, namely the large deviation theory, is therefore sometimes regarded as an extension of the law of large numbers and the central limit theorem [25]. To calculate the rate function of the WDF via the characteristic function of work, one applies the Gärtner-Ellis theorem as explained in the following [25].

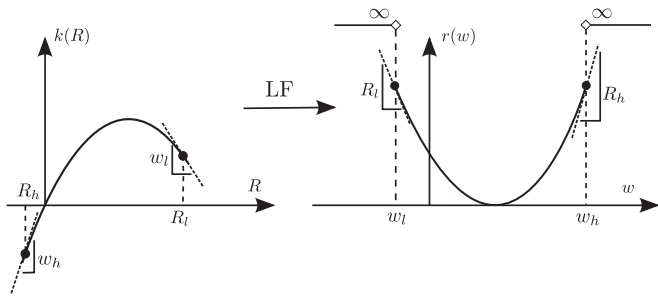


FIG. 2. Sketch of the Legendre-Fenchel (LF) transformation for the negative scaled cumulant generating function $c(R)$ for a single or double quench in the transverse field Ising model. At R_h and R_l , $c(R)$ takes on a linear form with slope w_h or w_l , respectively. These slopes and their positions determine the interval with finite values, as depicted on the right.

Setting $u = iR$, $R \in \mathbb{R}$ in Eq. (7), one can define the negative scaled cumulant generating function of w ,

$$c(R) = - \lim_{N \rightarrow \infty} \frac{1}{N} \ln G(R) \quad (25)$$

in analogy to the free-energy density in Eq. (21). If $c(R)$ exists, $G(R)$ is said to obey a large deviation principle, i.e., $G(R) \propto e^{-Nc(R)}$, with a rate function $c(R)$ [25]. Moreover, it follows that $c(R)$ is always concave and continuous inside the relevant domain of definition. The function $c(R)$ simplifies significantly, because $G(R)$ splits into products over k . Thus,

$$\begin{aligned} c(R) &= - \lim_{N \rightarrow \infty} \ln \prod_{0 < k < \pi} G_k(R) \\ &= - \lim_{N \rightarrow \infty} \sum_{0 < k < \pi} \ln G_k(R) \\ &= - \int_0^\pi \frac{dk}{2\pi} \ln G_k(R). \end{aligned} \quad (26)$$

Having showed the existence of $c(R)$, the Gärtner-Ellis theorem states that, if $c(R)$ is differentiable with respect to R , the probability distribution $p(w)$ also takes on the large deviation form. The corresponding rate function $r(w)$ is then obtained by a Legendre-Fenchel transformation [25] via

$$r(w) = - \inf_{R \in \mathbb{R}} [wR - c(R)]. \quad (27)$$

Here, the infimum is evaluated within the domain of definition of $c(R)$, which includes $R = \pm\infty$.

In Fig. 2, a sketch of the LF transformation is depicted to show how the shape of $c(R)$ determines the properties of $r(w)$. Despite the precise quantitative behavior, one can already deduce several generic features of $r(w)$ by analyzing $c(R)$. In the region where $c(R)$ is strictly concave, i.e., not even linear, there is a duality between the two related functions that transforms the slope \tilde{w} of $c(R)$ at position \tilde{R} into the slope \tilde{R} of $r(w)$ at position \tilde{w} and vice versa [25]. It follows that a function $c(R)$, which is strictly concave on the entire axis, would lead to a rate function that is not confined to some interval, because the positive and negative slopes are unbounded. While this can be the case for a free bosonic field theory [24], we expect a different behavior for the transverse field Ising model, as we will see shortly.

If the negative scaled cumulant generating function $c(R)$ has a linear asymptotic behavior, it is not strictly concave and the duality does not hold anymore. Let us assume that the slopes of $c(R)$ are bounded and have a maximal and minimal value, which are already reached for finite R as sketched in Fig. 2. Then, the LF transformation yields for the linear parts a negative infimum value that is infinite such that $p(w > w_h) = p(w < w_l) = 0$. Moreover, the rate function of the WDF will be finite at the boundaries as the linear behavior is not only asymptotically reached, but is reached for some finite R . Summing up, the expectation is to observe a rate function that has a similar shape to the sketch in Fig. 2 on the right.

Having explained how the shape of the rate function and its corresponding negative scaled cumulant generating function are mathematically related via the LF transformation, we still lack a physical motivation for why the rate function $r(w)$ should look as it is depicted. Indeed, there has to be a minimum and a maximum in the work density due to the fermionic properties of the system. Let us consider, for example, a first measurement where all k -sectors are in the highest state, i.e., the doubly occupied state, while a second measurement shows no sector is occupied. Then, the difference of the two measurements will represent the maximal energy that can be extracted from the system and therefore be the minimal possible work density. More energy cannot be extracted because there are no further fermions that could be excited initially. An analogous argument holds for the maximal work density.

In the following analysis, the rate functions for the single and double quench protocols are studied in detail. The results are obtained by numerically computing both the Legendre-Fenchel transformation in Eq. (27) and its argument, i.e., the integral in Eq. (26) over the analytic expression in Eqs. (18) or (19). The explicit time dependence that appears when considering the double quench protocol translates into a time-dependent $c(R, t)$ and finally $r(w, t)$.

A. Rate function for the single quench

The first part of the analysis concentrates on studying the single quench protocol. At $T = 0$, the minimal measurable work density is the difference of the ground-state energy densities of $H(g)$ and $H(g')$ given by $\Delta = \epsilon^0(g') - \epsilon^0(g)$ with

$$\begin{aligned} \epsilon^0(g) &= \frac{E^0(g)}{N} = - \frac{1}{N} \sum_{0 < k < \pi} \epsilon_k(g) \stackrel{N \rightarrow \infty}{=} - \frac{1}{2\pi} \int_0^\pi dk \epsilon_k(g) \\ &= - \frac{1+g}{\pi} \text{Ell}_2 \left(\frac{4g}{(1+g)^2} \right), \end{aligned} \quad (28)$$

and $\text{Ell}_2(x)$ denotes the elliptic integral of the second kind. Shifting w by Δ ensures that $w = 0$ corresponds to the smallest accessible work measurement such that $p(w < 0) = 0$. For the following analysis of the rate function at $T > 0$, this energy shift is always included to be able to compare the results.

First of all, one has to check for the differentiability of $c(R)$ such that the Gärtner-Ellis theorem is applicable. Since the argument of the logarithm of the respective integrand in Eq. (26) given by Eq. (18) is an analytic function without roots or poles if $T > 0$, this is valid.

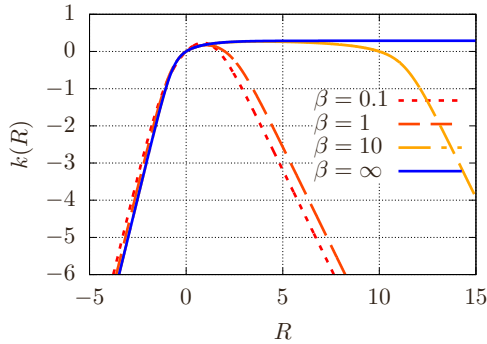


FIG. 3. Negative scaled cumulant generating function $c(R)$ of a single quench from $g = 0.5$ to $g' = 2$ at different inverse temperatures β . All functions at different nonzero temperature share an identical asymptotic behavior for $R \rightarrow \infty$ or $R \rightarrow -\infty$, respectively. It follows that the corresponding rate function is confined to an interval on the work density axis, as expected. When the temperature is very low, plateaus are created that become more pronounced with decreasing temperature until the zero-temperature limit (blue) shows an asymptote with vanishing slope for $R \geq \tilde{R}$. This ensures that $p(w < 0) = 0$.

The negative scaled cumulant generating function $c(R)$ for different inverse temperatures β is depicted in Fig. 3. Studying this function, we can already deduce its main features using the previous considerations. Except for the zero-temperature case, where the right asymptote has a slope equal to zero, the asymptotes of $c(R)$ at any other temperature share a common negative slope. This behavior is responsible for the rate function at $T = 0$ to be confined to values $w \geq 0$. On the left side, however, all temperatures have the same positive slope for $R \ll 0$. The analytical method to study the asymptotic behavior is the analysis of Eq. (26) for $R \rightarrow \pm\infty$. One finds that for $T > 0$,

$$c(R) \sim \begin{cases} 2\epsilon^0(g)R + C_\infty & \text{for } R \rightarrow \infty, \\ -2\epsilon^0(g')R + C_{-\infty} & \text{for } R \rightarrow -\infty \end{cases} \quad (29)$$

with constants $C_{\pm\infty}$ and (negative) ground-state energy densities $\epsilon^0(g)$ and $\epsilon^0(g')$. This directly translates into an identical upper bound for all rate functions $r(w)$ with any finite temperature and a common negative lower bound for all temperatures $T > 0$ (see Figs. 4 and 5). Consequently, it follows that at nonzero temperature,

$$p(w) = 0 \quad \text{for } w < 2\epsilon^0(g) \quad \text{and} \quad w > -2\epsilon^0(g').$$

In other words, it is possible that negative work can be measured if $T > 0$, although being highly improbable for very low temperatures. Microscopically, this can be realized by a quench where many initially excited k -sectors end up in states with lower energy, thus extracting energy from the system. This does not violate the second law of thermodynamics, since the mean value \bar{w} where $r(\bar{w}) = 0$ is always larger than 0. The limits in Eq. (29) show that the prequench parameter g determines the lower bound, while the postquench value g' determines the upper bound. This can be understood as follows: If, for example, the system begins in the highest excited state (all k -sectors are doubly occupied), the energy density is given as $\epsilon^h(g) = -\epsilon^0(g)$. To measure the minimal

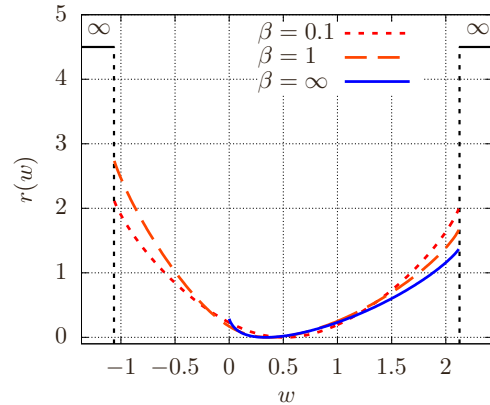


FIG. 4. The rate function $r(w)$ of the work distribution function for a single quench from $g = 0.5$ to $g' = 2$ at different inverse temperatures β . For nonzero temperatures, the rate function is finite within some interval determined by the ground-state energy densities of the pre- and postquench Hamiltonian. For larger or smaller work densities, the rate function is infinite (black lines) such that the corresponding work distribution function vanishes. The $T = 0$ ($\beta = \infty$, blue line) case shows a peculiarity: The rate function is already infinite for $w < 0$, such that $p(w < 0) = 0$. This results from the fact that initially only the ground state of the prequench Hamiltonian is occupied.

work, one needs to extract maximal energy from the system, which can be achieved by quenching the system to the ground state of the postquench Hamiltonian with energy $\epsilon^0(g')$. The difference (including the energy shift by subtracting Δ) yields $w_{\min} = \epsilon^0(g') - [-\epsilon^0(g)] - \Delta = 2\epsilon^0(g)$. An analogous explanation holds for the upper bound.

B. Rate function for the double quench

In the mentioned work about the DPT, Heyl *et al.* computed the rate function of the work distribution function for a

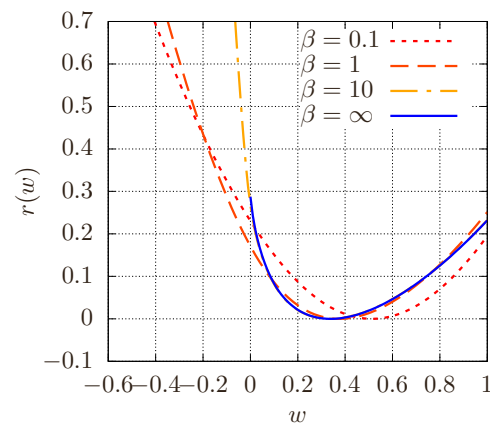


FIG. 5. Zoom into Fig. 4 showing the rate function $r(w)$ of the work distribution function for a single quench from $g = 0.5$ to $g' = 2$ at different inverse temperatures β . In addition to the previous data, the curve for $\beta = 10$ has been added to demonstrate the steep ascent of the rate function for low temperatures. One notices that the difference between the low-temperature and zero-temperature results is already too small to be adequately resolved.

double quench at zero temperature and showed that the DPT is intrinsically included in this quantity [10]. In this way, interpreting the Loschmidt echo as the probability density that zero work is performed, the work distribution function can be regarded as a generalization of the Loschmidt echo. Their study also used the Gärtner-Ellis theorem to compute the rate function $r(w, t)$ by transforming the corresponding negative scaled cumulant generating function $c(R, t)$ via a Legendre-Fenchel transformation as explained earlier. For $R = \infty$, the latter quantity shows nonanalyticities for quenches across the QCP $g_c = 1$ at the critical times $t_n^* = t^*(n + \frac{1}{2})$, $n = 0, 1, 2 \dots$ and momentum k^* . This behavior extends to the rate function if $w = 0$, thus rendering $r(w = 0, t)$ nonanalytic. Now, a similar procedure will be used to investigate whether a DPT can also occur at nonzero temperatures by analyzing the corresponding negative scaled cumulant generating function $c(R, t)$. If this function features nonanalytic behavior, it will continue to the LF-transformed version, i.e., the rate function. As for the single quench, one therefore studies the argument of the logarithm in the integrand in Eq. (26) given by Eq. (19) for possible roots when $u = iR$ with $R \in \mathbb{R} \cup \{-\infty, \infty\}$. However, in contrast to the $T = 0$ case, we will now show that the integrand is always analytic no matter what quench parameters are considered. This can be seen by examining the denominator and numerator in Eq. (19) more closely. For $\beta < \infty$ ($T > 0$), both are strictly positive since only positive terms are added. The canonical distribution of initial states represented by the $\cosh[\beta E_k(g)]$ terms inhibits the existence of roots in any form. In fact, the expression is everywhere analytic as in the single quench case for $T > 0$. It follows that nonanalyticities and therefore dynamical phase transitions as in the understanding of Heyl *et al.* cannot occur under any conditions if $T > 0$ in the transverse field Ising model. To clarify this difference and to compare to the zero-temperature results, we now study the integrand at the critical times t_n^* and critical momentum k^* . For this mode, $2\phi_{k^*} = \pi/2$ and the argument of the logarithm in the integrand becomes

$$G_{k^*}(R, t_n^*) = \frac{1 + \cosh[(-2R + \beta)\epsilon_{k^*}(g)]}{1 + \cosh[\beta\epsilon_{k^*}(g)]}. \quad (30)$$

This term can only vanish in the zero-temperature limit $\beta \rightarrow \infty$,

$$\lim_{\beta \rightarrow \infty} G_{k^*}(R, t_n^*) = e^{-2R\epsilon_{k^*}(g)} \quad (31)$$

for $R \rightarrow \infty$. Since this is the argument of the logarithm in the integrand, this exactly recovers the appearance of nonanalytic behavior as shown in Ref. [10]. However, for any nonzero temperature, the right-hand side of Eq. (30) cannot be zero and therefore DPTs in the sense of Heyl *et al.* are not possible. The asymptotic behavior of $c(R, t)$ is again determined by the ground-state energy densities of the initial and final Hamiltonian, which are identical for a double quench, i.e., $H(g)$, such that

$$c(R, t) \sim \begin{cases} 2\epsilon^0(g)R + C_\infty & \text{for } R \rightarrow \infty, \\ -2\epsilon^0(g)R + C_{-\infty} & \text{for } R \rightarrow -\infty. \end{cases} \quad (32)$$

Similarly as before, it follows that $p(w) = 0$ everywhere except for $2\epsilon^0(g) \leq w \leq -2\epsilon^0(g)$.

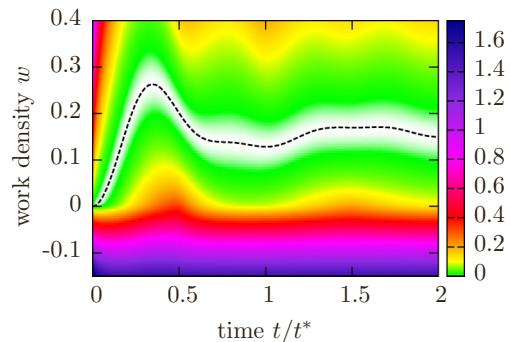


FIG. 6. Rate function $r(w, t)$ for a double quench from $g = 0.5$ to $g' = 2$ and back to g after time t at inverse temperature $\beta = 10$ in a color-coded form. The dashed line depicts the expectation value of the performed work, i.e., where $r(w, t) = 0$. In contrast to the zero-temperature version of this plot, the work density plane is extended to negative work densities. This results from the initial canonical distribution of states, i.e., the inclusion of excited states, such that energy is extracted from the system when the final state is energetically lower than the initial one. However, in contrast to positive work densities, the ascent of $r(w, t)$ is much steeper for $w < 0$ similar to the single quench in Fig. 5. The red areas around $t/t^* = 0.5$ and 1.5 are remnants of the dynamical phase transition at $T = 0$, as can be seen in direct comparison and by analyzing the constant work density cuts in Fig. 7.

Figure 6 shows the result for the rate function $r(w, t)$ of a double quench protocol across the QCP with identical parameters as in Ref. [10], but for a low, nonzero temperature. Comparing this result with its zero-temperature correspondence shown in Fig. 2 in Ref. [10], one immediately notices the general qualitative agreement in shape. The expectation value where $r(w, t) = 0$ (indicated by the dashed line) continues to be shifted toward higher work densities at times $t_1^* = 0.5$ and $t_2^* = 1.5$, despite the absence of a DPT. The new feature is the expected extension to negative work densities, which seem to be not as heavily influenced by the DPT as the positive part and

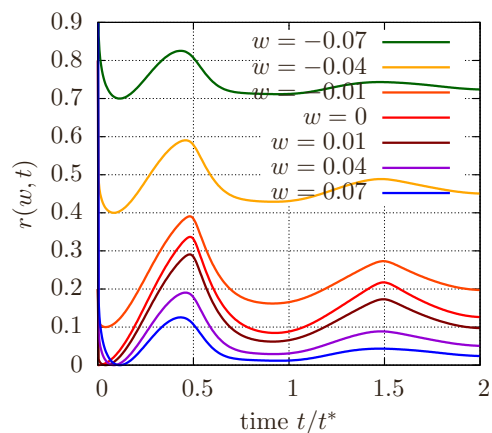


FIG. 7. Various cuts of the rate function plot in Fig. 6 for fixed values of the work density w (w increases from top to bottom). While the rate function of the Loschmidt echo ($w = 0$) at $T = 0$ features DPTs visible as kinks, its nonzero temperature equivalent is perfectly smooth. However, the DPT still heavily influences the behavior of the rate function in the form of a shift to larger values of $r(w, t)$.

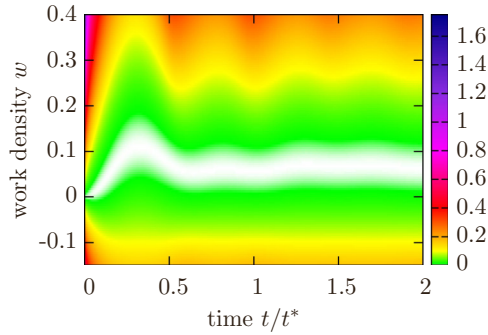


FIG. 8. Rate function $r(w,t)$ for a double quench from $g = 0.5$ to $g' = 2$ and back to g after time t at inverse temperature $\beta = 1$ in a color-coded form. The higher temperature leads to a flatter behavior of the expectation value compared to $\beta = 10$, while the rate functions for fixed times broaden and now almost equally extend to negative w . In other words, the rate function of the work distribution function becomes more symmetric with respect to the $w = 0$ axis with increasing temperature. This is understood to be a result of the initial canonical distribution where the energy levels become more evenly populated as T grows.

display a steep ascent with decreasing w as in the single quench case. It is possible that the large slope undermines the visible effects of the DPT. Horizontal cuts of the plot for fixed values w are depicted in Fig. 7. At zero temperature, the $w = 0$ line represents the rate function of the Loschmidt echo and features the DPT through kinks at the specified times t_n^* . If $T > 0$, these kinks cease to exist, as expected, and the rate function $r(w = 0, t)$ is smooth. With increasing temperature, the effect of the DPT at $T = 0$ diminishes, as can be seen in Fig. 8. A higher temperature means that the canonical distribution is more uniformly distributed such that the number of energy extraction and insertion transitions equalizes. As a consequence, the rate function becomes more symmetric around the expectation value, which approaches the $w = 0$ line. The only visible remnant of the DPT is the slightly shifted rate functions in the vicinity of $t/t^* \approx 0.25$. In comparison to lower temperatures, it appears that this area has also moved to earlier times.

V. THE TASAKI-CROOKS-JARZYNSKI THEOREM

In this section, we study the one-dimensional transverse field Ising model in the context of a famous fluctuation relation, namely the Tasaki-Crooks-Jarzynski relation. In general, fluctuation theorems provide additional information about the statistical properties of the physical quantity of interest and become important whenever a statistical description is needed for a complete characterization [5]. This is the case, for example, when work measurements are considered due to the initial distribution of states at a certain temperature. One famous achievement in this context was certainly the Jarzynski equality given by

$$\langle e^{-\beta W} \rangle_\lambda = e^{-\beta \Delta F} \tag{33}$$

in its quantum form for a ramp protocol λ , where the average is taken with respect to the initial Gibbs distribution [26–28]. It means that the mean of exponentiated work values W of many identical experiments equals the exponentiated change

of the free energy ΔF of the corresponding equilibrium states. The impact of this theorem relies on the fact that it also holds for nonequilibrium work measurements. One can therefore learn about the change of the free energy of the equilibrium states even if the system is not in equilibrium during the work measurements. A more general theorem including Eq. (33) is the Tasaki-Crooks-Jarzynski relation, which relates the work distribution functions of a quench process λ and its time-inverted version $\tilde{\lambda}$ to the change of the equilibrium Gibbs free energy ΔF . It reads

$$\frac{p[w; \lambda]}{p[-w, \tilde{\lambda}]} = e^{N\beta(w - \Delta f)}, \tag{34}$$

where $p[w; \lambda]$ denotes the work distribution function of the work density w , N is the system size, and $\Delta f = \Delta F/N$ is the free-energy density [29–31].

A. Single quench

Rewriting Eq. (34) in terms of its rate functions of the forward (F) and backward (B) quench produces a remarkable result: the Tasaki-Crooks-Jarzynski relation naturally translates into a simple algebraic equation independent of the system size N , namely

$$\frac{1}{N} \ln \left(\frac{p_F(w)}{p_B(-w)} \right) = r_B(-w) - r_F(w) = \beta(w - \Delta f). \tag{35}$$

This form offers an easy way to measure Δf , as already shown in experiments [6–8]. According to the equation above, it is even possible to “read off” the value for Δf in the plot that is shown in Fig. 9. The result can be verified with an exact calculation with the free-energy density,

$$\begin{aligned} f(g) &= -\frac{1}{N\beta} \ln Z(g) = -\frac{1}{N\beta} \prod_{0 < k < \pi} \{2 + 2 \cosh [\beta E_k(g)]\} \\ &= -\frac{1}{2\pi\beta} \int_0^\pi dk \ln \{2 + 2 \cosh [\beta E_k(g)]\}. \end{aligned} \tag{36}$$

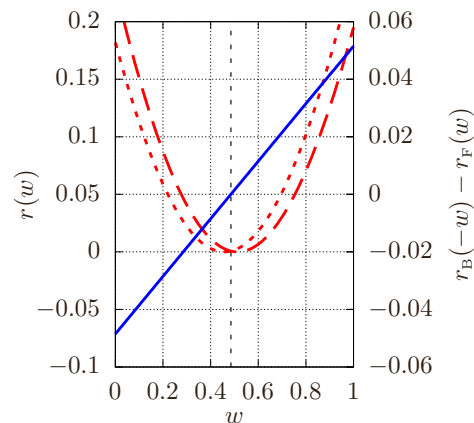


FIG. 9. Rate functions $r(w)$ for a single quench from $g = 0.5$ to $g' = 2$ (red dash-dotted line) and its time-reversed counterpart (red dotted) at temperature $\beta = 0.1$. The difference of the rate functions shows linear behavior (blue solid) and allows us to directly determine Δf . The black vertical line (dashed) depicts the exact calculation using Eq. (36).

Within numerical accuracy, both methods show the expected perfect agreement.

Beyond numerics, the Tasaki-Crooks-Jarzynski relation can be verified exactly using the Fourier-transformed version of Eq. (34) [5],

$$Z(g)G_F(u) = Z(g')G_B(-u + i\beta). \quad (37)$$

On both sides, the partition function Z cancels with itself when plugging in $G(u)$ as in Eq. (14) such that only the products over k remain. It follows that the equation above reduces to a k -sector-like form. After dividing by 2 on both sides, it now reads

$$\begin{aligned} & 1 + \cosh[(iu + \beta)\epsilon_k(g)] \cos[u\epsilon_k(g')] \\ & - i \sinh[(iu + \beta)\epsilon_k(g)] \cos(2\phi_k) \sin[u\epsilon_k(g')] \\ & = 1 + \cosh\{[i(-u + i\beta) + \beta]\epsilon_k(g')\} \cos[(-u + i\beta)\epsilon_k(g)] \\ & - i \sinh\{[i(-u + i\beta) + \beta]\epsilon_k(g')\} \cos(-2\phi_k) \\ & \times \sin[(-u + i\beta)\epsilon_k(g)]. \end{aligned} \quad (38)$$

In the next step, one simply uses the trigonometric identities $\cosh(\pm ix) = \cos(x)$ and $\sinh(\pm ix) = \sin(\pm x)$ with $x \in \mathbb{C}$ to show that the right-hand side recovers the left-hand side. Note that the minus sign in $\cos(-2\phi_k)$, which results from the backward protocol $g' \rightarrow g$, is canceled due to the symmetry relation of the cos function.

B. Double quench

For the double quench, Eq. (34) simplifies immediately because the forward and the backward quench are identical, i.e., the protocol describes a *cyclic process*. Consequently, $\Delta F = 0$ and the equation relates the region $r(w \geq 0)$ to the $r(w < 0)$ part:

$$r(w) + \beta w = r(-w). \quad (39)$$

It follows that knowing one part of the entire rate function $r(w, t)$ in Fig. 6 is sufficient, because the other part is determined by it. In particular, the region where $w < 0$ and the rate function strongly ascends is difficult to address experimentally. With the help of Eq. (39), it would only be necessary to measure the part where the work measurements take on positive values. The numerical verification of the Tasaki-Crooks-Jarzynski relation is shown in Fig. 10, where the agreement between the left- and right-hand side of Eq. (39) is displayed. Analogously to the single quench analysis, one can verify the Tasaki-Crooks-Jarzynski theorem exactly via its Fourier-transformed version. Due to the simple symmetric form of the ramp protocol, the partition functions on the left and right side of Eq. (37) are identical. One can therefore immediately study the final form of the characteristic function of work given in Eq. (19) and check whether it is identical for u and $-u + i\beta$. The only part where u appears is the cosh term, and since

$$\cosh[(2iu + \beta)\epsilon_k(g)] = \cosh\{[2i(-u + i\beta) + \beta]\epsilon_k(g)\}, \quad (40)$$

the identity is shown.

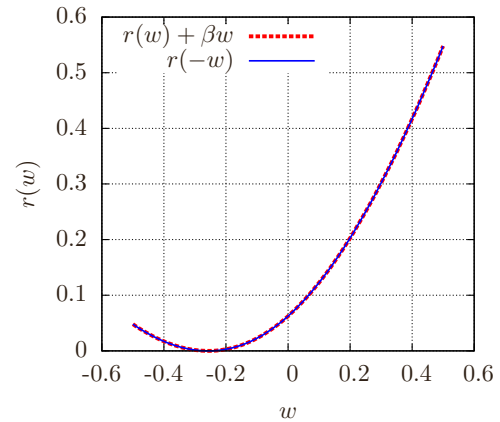


FIG. 10. Rate function $r(-w)$ and $r(w) + \beta w$ for a double quench from $g = 0.5$ to $g' = 2$ and the inverse temperature $\beta = 2$, which are identical. From the Tasaki-Crooks-Jarzynski theorem, it follows that both rate functions are related via the additional summand βw , such that $r(w \geq 0, t)$ determines $r(-w, t)$ and vice versa.

VI. CONCLUSIONS

In this paper, we demonstrated analytically that DPTs in the one-dimensional transverse field Ising model cannot occur at nonzero temperatures due to the initial distribution of states being thermal. To show this, we calculated the characteristic function of work for the simple single and double quench protocol. Due to the large deviation form of this function, it was possible to compute the rate function of the work distribution function via a Legendre-Fenchel transformation. We elucidated how the quench parameters define the limits of the rate function in the context of this transformation. Despite the lack of nonanalyticities, the work distribution function at $T > 0$ was shown to be continuously influenced by the DPT at $T = 0$. In the quantitative study, we displayed how this influence diminishes with increasing temperature and the rate function changes accordingly. This observation in one dimension can be contrasted with the results of Canovi *et al.*, who found nonanalytic behavior even at nonzero temperatures in the Falicov-Kimball model and the Hubbard model in the dynamical mean-field limit (DMFT) [16]. We attribute this difference to the generic behavior of low-dimensional quantum models in which quantum fluctuations become more pronounced and generically suppress nonanalytic behavior.

In the final section, we discussed and analytically verified the Tasaki-Crooks-Jarzynski theorem for a global single and double quench in the chosen system. Here, the numerical study focused on the applicability of the Tasaki-Crooks-Jarzynski relation for different practical purposes.

ACKNOWLEDGMENTS

This work was supported through CRC 1073 (Project B03) of the Deutsche Forschungsgemeinschaft (DFG). We are grateful to M. Schmitt and D. Fioretto for a careful reading of the manuscript and valuable discussions.

- [1] A. Polkovnikov, K. Sengupta, A. Silva, and M. Vengalattore, *Rev. Mod. Phys.* **83**, 863 (2011).
- [2] T. Kinoshita, T. Wenger, and D. S. Weiss, *Nature (London)* **440**, 900 (2006).
- [3] M. Greiner, O. Mandel, T. Esslinger, T. W. Hänsch, and I. Bloch, *Nature (London)* **415**, 39 (2002).
- [4] P. Talkner, E. Lutz, and P. Hänggi, *Phys. Rev. E* **75**, 050102 (2007).
- [5] M. Campisi, P. Hänggi, and P. Talkner, *Rev. Mod. Phys.* **83**, 771 (2011).
- [6] J. Liphardt, S. Dumont, S. B. Smith, I. Tinoco, and C. Bustamante, *Science* **296**, 1832 (2002).
- [7] D. Collin, F. Ritort, C. Jarzynski, S. Smith, I. Tinoco, and C. Bustamante, *Nature (London)* **437**, 231 (2005).
- [8] F. Douarche, S. Ciliberto, A. Petrosyan, and I. Rabbiosi, *Europhys. Lett.* **70**, 593 (2005).
- [9] S. An, J.-N. Zhang, M. Um, D. Lv, Y. Lu, J. Zhang, Z.-Q. Yin, H. T. Quan, and K. Kim, *Nat. Phys.* **11**, 193 (2015).
- [10] M. Heyl, A. Polkovnikov, and S. Kehrein, *Phys. Rev. Lett.* **110**, 135704 (2013).
- [11] A. Silva, *Phys. Rev. Lett.* **101**, 120603 (2008).
- [12] C. Karrasch and D. Schuricht, *Phys. Rev. B* **87**, 195104 (2013).
- [13] J. N. Kriel, C. Karrasch, and S. Kehrein, *Phys. Rev. B* **90**, 125106 (2014).
- [14] S. Vajna and B. Dóra, *Phys. Rev. B* **89**, 161105 (2014).
- [15] F. Andraschko and J. Sirker, *Phys. Rev. B* **89**, 125120 (2014).
- [16] E. Canovi, P. Werner, and M. Eckstein, *Phys. Rev. Lett.* **113**, 265702 (2014).
- [17] M. Fagotti, [arXiv:1308.0277](https://arxiv.org/abs/1308.0277) [cond-mat.stat-mech].
- [18] M. Heyl, *Phys. Rev. Lett.* **113**, 205701 (2014).
- [19] M. Heyl, *Phys. Rev. Lett.* **115**, 140602 (2015).
- [20] D. Andrieux and P. Gaspard, *Phys. Rev. Lett.* **100**, 230404 (2008).
- [21] P. Smacchia and A. Silva, *Phys. Rev. E* **88**, 042109 (2013).
- [22] S. Sachdev, *Quantum Phase Transitions*, 2nd ed. (Cambridge University Press, Cambridge, 2011).
- [23] E. Lieb, T. Schultz, and D. Mattis, *Ann. Phys. (NY)* **16**, 407 (1961).
- [24] A. Gambassi and A. Silva, *Phys. Rev. Lett.* **109**, 250602 (2012).
- [25] H. Touchette, *Phys. Rep.* **478**, 1 (2009).
- [26] C. Jarzynski, *Phys. Rev. Lett.* **78**, 2690 (1997).
- [27] C. Jarzynski, *Eur. Phys. J. B* **64**, 331 (2008).
- [28] C. Jarzynski, in *Time*, Progress in Mathematical Physics Vol. 63, edited by B. Duplantier (Springer, Basel, 2013), pp. 145–172.
- [29] G. E. Crooks, *Phys. Rev. E* **60**, 2721 (1999).
- [30] H. Tasaki, [arXiv:cond-mat/0009244](https://arxiv.org/abs/cond-mat/0009244).
- [31] J. Kurchan, [arXiv:cond-mat/0007360](https://arxiv.org/abs/cond-mat/0007360).